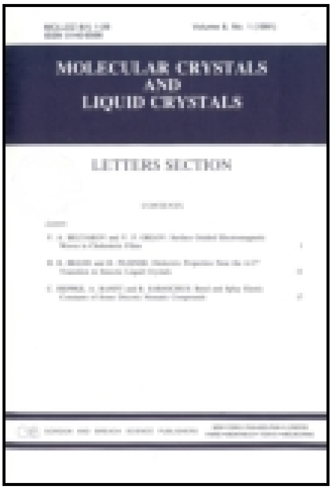

Molecular Crystals and Liquid Crystals
Publication details, including instructions for authors and subscription information:
http://www.tandfonline.com/loi/gmcl20

High-Performance Printed Organic Ambipolar Complementary Inverters with Polyazine Containing Diketopyrrolopyrrole

Won-Tae Park[a], Seok-Ju Kang[a] & Yong-Young Noh[a]
[a] Department of Energy and Materials Engineering, Dongguk University, Seoul, Republic of Korea
Published online: 17 Nov 2014.

Mol. Cryst. Liq. Cryst., Vol. 600: pp. 123–128, 2014

ISSN: 1542-1406 print/1563-5287 online
DOI: 10.1080/15421406.2014.936800

High-Performance Printed Organic Ambipolar Complementary Inverters with Polyazine Containing Diketopyrrolopyrrole

WON-TAE PARK, SEOK-JU KANG, AND YONG-YOUNG NOH*

Department of Energy and Materials Engineering, Dongguk University, Seoul, Republic of Korea

We report ambipolar organic field effect transistors (OFETs) and complementary inverters based on polyazine containing diketopyrrolopyrrole (PBTDAZ). PDBTAZ OFETs showed well-balanced electron and hole mobilities of 0.13 and 0.12 cm^2/(V·s) at a low annealing temperature of 100^{o}C using bottom-contact, top-gate geometry with a CYTOP^{TM} gate dielectric layer. The mobilities were improved to 0.56 cm^2/(V·s) by thermal annealing (150°C). The ambipolar complementary-inverter-based PDBTAZ OFETs showed ideal V_{inv} near half of V_{DD} with a high gain of 15~20 due the well-balanced electron and hole mobilities.

Keywords Organic field-effect transistors; conjugated molecules; ambipolar semiconductor; complementary inverter

1. Introduction

Solution-processed π-conjugated polymers have drawn tremendous interest for use as an active element in organic field effect transistors (OFETs) for large-area and flexible electronic applications such as a back plane driver in flexible displays, integrated circuits in printed RFID tags, or various sensors with cost-effective printing processes [1–2]. Even though impressive progress has been made for the past decade in polymer integrated circuits (ICs), many hurdles must still be overcome to realize commercial products including printed polymer ICs, including a relatively low charge carrier mobility of conjugated polymers, difficulty in achieving high resolution by printing processes for patterning, and an absence of large-area coating methods for thin film deposition [3]. In addition, to improve the characteristics of printed polymer ICs, complementary inverters composed of both one n- and p-channel transistors should been applied as basic building blocks, because of their advantages over unipolar inverters of low power consumption and high noise margin [4–5].

To realize complementary polymer ICs, n- and p-channel regions must be patterned. Therefore, various novel patterning methods have been reported to replace the conventional

*Address correspondence to Yong-Young Noh, Department of Energy and Materials Engineering, Dongguk University, 26 Pil-dong, 3-ga, Jung-gu, Seoul 100-715, Republic of Korea. Tel.: +82-2-2260-4974; Fax: +82-2-2269-9649. E-mail: yynoh@dongguk.edu

Color versions of one or more of the figures in the article can be found online at www.tandfonline.com/gmcl.

photolithography process [6–8]. Inkjet printing is being considered as a promising patterning process, since depositing and patterning conjugated polymers have been done at the same time. We have reported polymer complementary ICs by inkjet printing n-type and p-type conjugated polymer solution on pre-patterned Au source/drain electrodes [9]. The printed polymer complementary ring oscillators showed a high operating frequency of ∼40 KHz. Another interesting approach is using ambipolar conjugated polymers as the active layer of complementary ICs. The ambipolar polymers enable the realization of complementary ICs by a simple blanket coating without patterning processes, since the single polymer can transport both electrons and holes efficiently. By doing this, process steps and material waste can also be reduced further. Recently, several interesting ambipolar conjugated polymers have been reported [10]. Low-bandgap donor-acceptor-type polymers based on diketopyrrolopyrole (DPP) have emerged as a promising class of materials exhibiting relatively high hole and electron mobilities [11]. The DPP acceptor core constitutes a planar moiety capable of forming π-π stacks in the solid state, leading to efficient charge transport through between polymer chains. Efficient transport of both electrons and holes allows for the fabrication of complementary ICs based on ambipolar transistors, which combine the robustness and good noise margin of truly complementary ICs with the ease of processing of unipolar logics. To improve the switch speed of ambipolar complementary ICs, not only a high mobility value but also good balance of electron and hole mobility is required.

We report solution-processable polymer ambipolar OFETs and inverters based on polyazine containing diketopyrrolopyrrole (PBTDAZ). PDBTAZ OFETs showed well-balanced electron and hole mobilities of 0.12 and 0.13 $cm^2/(V \cdot s)$, respectively, in bottom-contact, top-gate geometry with CYTOP^{TM} polymer gate dielectrics. The electron and hole mobilities were improved to 0.4 and 0.32 $cm^2/(V \cdot s)$ by thermal post annealing at 250°C. We have demonstrated printed polymer ambipolar inverters by a simple one-time spin coating without any sophisticated patterning techniques for the semiconducting layer. The ambipolar complementary-like inverters showed a high voltage gain of ∼23 at an inverting voltage of ±40.

2. Experimental

A. OFET Fabrication

Corning Eagle XG glass substrates were cleaned sequentially in sonication baths of acetone, isopropanol, and deionized water for 10 min each. The device source/drain (S/D) electrode was patterned by conventional lift-off photolithography processes. Au and Cr (thickness: 13 nm/2 nm) were used as source and drain metal electrodes. Ambipolar PDBTAZ was synthesized and used without any further purification. The details of the polymer synthesis were published elsewhere [12]. These semiconductors were dissolved in anhydrous chlorobenzene (Sigma Aldrich) to obtain a 4 mg/ml solution and were spin coated at 1400 rpm for 60 s and then thermally annealed at temperatures ranging from 100°C to 250°C for 20 min to obtain ∼38-nm-thick thin film in an N_2-purged glove box. CYTOP^{TM} (Asahi Glass, 809-M) with a CYTOP:CYTOP solvent ratio of 2:1 was used as a gate dielectric and spin-coated at 2000 rpm for 60 s and then baked at 100°C for 20 min in an N_2-purged glove box (thickness: 380 nm, Capacitance: 4.89 nF/cm^2). The transistors were completed by depositing the top gate electrodes (Al) via thermal evaporation using a metal shadow mask.

B. Complementary Inverter Fabrication and Characterization

The inverter fabrication used a shared one-output-line two-transistor pattern. This device pattern was fabricated on Corning Eagle XG glass by conventional lift-off photolithography

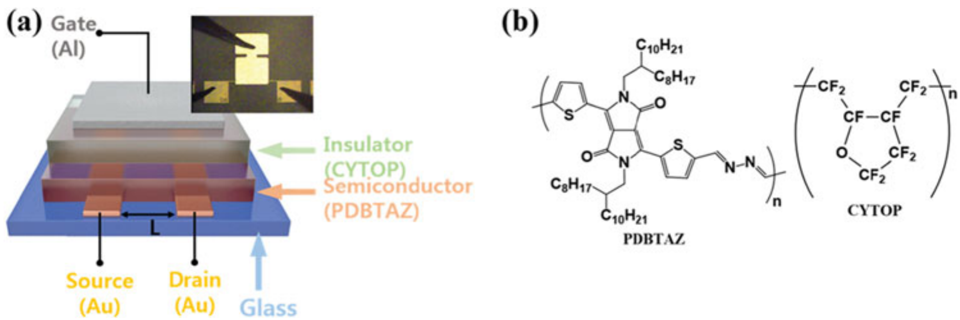

Figure 1. (a) Schematic illustration of top gate/bottom contact device structure. (b) Chemical structure of PDBTAZ and CYTOP™ chemical structure

processes. The formed functional electrical layer, PDBTAZ, and CYTOP were spin coated. The inverters were completed by depositing the two-transistor channel covered gate electrodes (Al) via thermal evaporation using a metal shadow mask. It works like a complementary circuit structure. The electrical characteristics of the OFETs were extracted from the drain current level via the gate voltage bias or drain voltage bias (channel width (W)/length (L): 1000/20 um). The static characteristics of the complementary inverters were extracted from the output line voltage transfer via the gate voltage bias and drain voltage (n:p channel ratio: 1:1; channel W/L: 1000/20 um). All measurements were taken using an Agilent HP4156A semiconductor parameter analyzer in an N_2-purged glove box.

3. Results and Discussion

Figure 1 shows the structure of the staggered top-gated/bottom-contact (TG/BC) OFETs and the molecular structure of the PDBTAZ and CYTOP used in the study. The highest occupied molecular orbital (HOMO) energetic level of PDBTAZ was 5.67 eV, which was measured by cyclovoltametry. The optical band gap was 1.43 eV [12]. The OFET characteristics were simply controlled by the thermal annealing temperature. The saturation mobilities (μ_{sat}) of PDBTAZ OFETs were calculated by conventional gradual channel approximation:

$$\mu_{sat} = \frac{2L}{C_{die} W V_{DS}} \left(\frac{\partial \sqrt{I_D}}{\partial V_{GS}} \right)^2 \quad (1)$$

for $|V_{DS}| > |V_{GS}\text{-}V_{TH}| > 0$ (saturation regime) where C_{die} is the gate dielectric capacitance per unit area, L is the channel length, W is the channel width, I_D is the drain current, V_{DS} is the drain-source voltage at the current I_D saturates, and V_{GS} is the gate-source voltage.

As shown in Figure 2, the characteristics of PDBTAZ OFETs depend on the post annealing temperature. The average hole and electron mobilities of PDBTAZ were increased by almost three times from 0.12 to 0.32 $cm^2/(V{\cdot}s)$ and 0.13 to 0.41 $cm^2/(V{\cdot}s)$ at 250°C, respectively. In addition, the threshold voltage (V_{TH}) was shifted by approximately 3.8 and 1.1 V for p- and n-type OFETs with an increase of the annealing temperature from 100 to 250°C. All device parameters such as the electron and hole mobility, V_{TH}, and subthreshold swing are summarized in Table 1. This improvement in charge carrier mobilities is essentially due to the better arrangement of polymer chains in the film, the reduced d-spacing, and the increased crystallites at the higher annealing temperature, which were not present in the as-spun PDBTAZ films [13]. PDBTAZ OFETs showed a large contact resistance

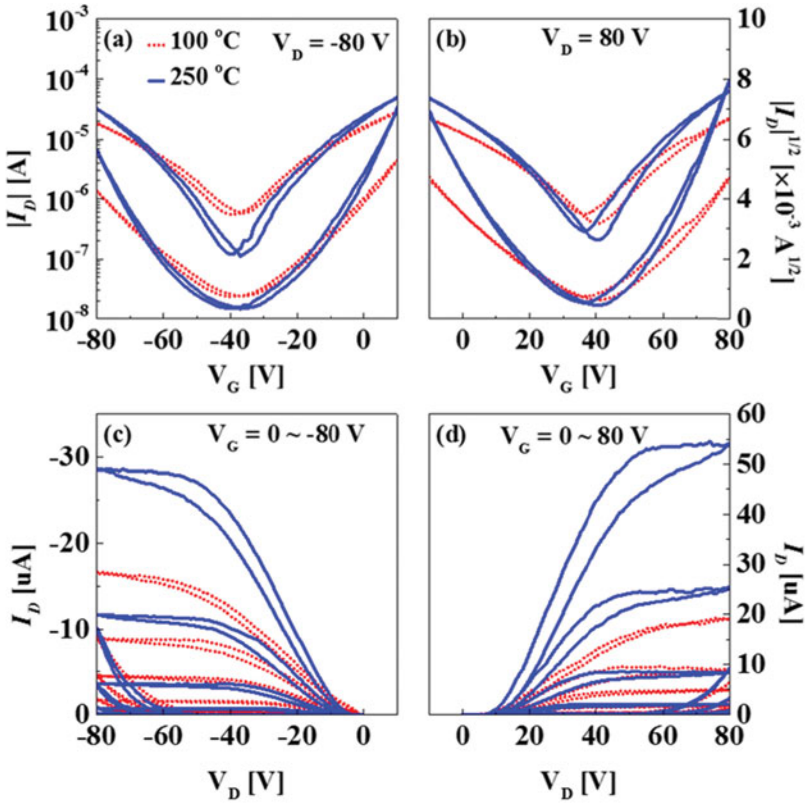

Figure 2. Transfer and output characteristics of PDBTAZ thin film annealed at 100°C (dotted line) and 250°C (solid line) at $V_D = -80$ V [(a) and (c)] and $V_D = 80$ V [(b) and (d)].

Table 1. TG/BC OFET parameters for PDBTAZ with various OSC annealing temperature

T_a (a) °C		$\mu_{sat, aver.}$ (b) [cm^2/(V·s)]	$V_{Th, aver.}$ (c) [V]	$SS_{aver.}$ (d) [V/dec.]	Inverting voltage (e) [V]	$Gain_{max}$ (f)
100	Hole	0.12	−40.91	−34.01	39	16.43
	Electron	0.13	40.89	29.59		
150	Hole	0.20	−54.14	−15.00	37	22.87
	Electron	0.56	45.43	18.57		
200	Hole	0.13	−50.46	−22.38	28	22.61
	Electron	0.33	42.39	18.96		
250	Hole	0.32	−44.71	−21.24	39	19.82
	Electron	0.41	42.02	21.00		

(a) Annealing temperature (b), (c) Calculated from the plot of $I_D^{1/2}$ versus V_G according to the saturation current equation. (d) Calculated from the plot of log(abs(I_D)) versus V_G according to the subthreshold slope equation. *3∼8sample average data (e) Inverting output voltage point (f) Maximum value of $-dV_{out}/dV_{in}$ at $V_{DD} = +80$ V.

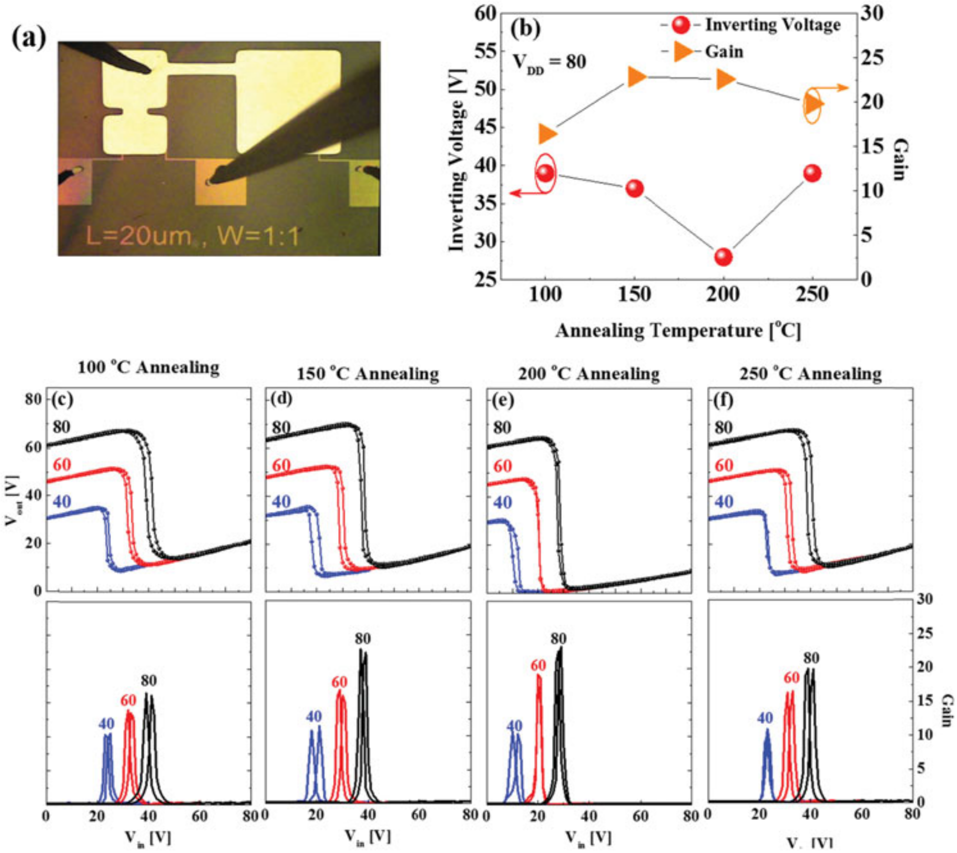

Figure 3. (a) Microscope image and (b) inverting voltage and gain versus annealing temperature of TG/BC PDBTAZ inverters. (c)–(f) Voltage transfer curves and gain versus V_{in} at 100, 150, 200, and 250°C annealing temperature.

even after high-temperature thermal annealing mainly due to a large barrier height (0.5–1 eV) for hole and electron injection from the Au source/drain electrodes.

To clarify the effect of differences in the electron and hole mobility on the inverter characteristics, we have fabricated and measured a TG/BC PDBTAZ inverter, as shown in Fig. 3 (a). Table 1 shows that the post-annealed PDBTAZ OFETs at 100 and 250°C showed similar electron and hole mobility. Therefore, the inverting voltage (V_{inv}) of both devices exhibited an ideal value near half (40 V) of the supply voltage (V_{DD}) = 80 V ($\frac{1}{2}V_{DD}$) with a high gain of 15 to 20 [see Fig. 3(b)]. On the other hand, annealed devices at 200°C showed a large shifted V_{inv} of 27.5 V from $\frac{1}{2}V_{DD} = 40$ V because of a large difference of electron [0.33 $cm^2/(V{\cdot}s)$] and hole mobility [0.13 $cm^2/(V{\cdot}s)$] in ambipolar PDBTAZ OFETs. V_{inv} and the gain of all measured ambipolar PDBTAZ inverters are also summarized in Table 1. As shown in Figs. 3 (c)–(f), the ambipolar complementary inverters based on the ambipolar PDBTAZ OFETs and Au contacts exhibit Z-shaped-like voltage transfer curves (VTC). The output voltage (V_{out}) deviates from the V_{DD} at a low input voltages (V_{in}) due to the efficient hole transport in the pull-down transistor, thus strongly reducing its impedance. For larger V_{in}, the VTC curves also exhibit some deviation from zero V_{out} due to the electron transport in the pull-up transistor in the ambipolar inverter. This is mainly attributed to the leakage current through the pull-down (or pull-up) transistor when the pull-up or pull-down transistor turns on. The abnormal Z-shaped characteristics in ambipolar inverters can be effectively improved by insertion of a charge injection and blocking layer between the semiconducting layer and source/drain electrode [14].

4. Conclusion

We have successfully demonstrated ambipolar OFETs and complementary inverters with PDBTAZ by cost-effective solution processes. The ambipolar PDBTAZ OFETs exhibited well-balanced electron and hole mobilities of 0.13 and 0.12 $cm^2/(V\cdot s)$, respectively, at a low annealing temperature of 100°C. The mobilities were improved to 0.56 $cm^2/(V\cdot s)$ by a thermal annealing process. The ambipolar complementary-inverter-based PDBTAZ OFETs showed ideal V_{inv} near half of V_{DD} with a high gain of 15–20 due to the well-balanced electron and hole mobilities.

Funding

This research was financially supported by the Pioneer Research Center Program through the National Research Foundation of Korea funded by the Ministry of Science, ICT & Future Planning (NRF-2013M3C1A3065528), and by the Dongguk University Research Fund of 2013.

References

[1] Zaumseil, J., & Sirringhaus, H. (2007). *Chem Rev.*, *107*, 1296.
[2] Noh, Y. Y., Zhao, N., Caironi, M., & Sirringhaus, H. (2007). *Nat. Nanotech.*, *2*, 784.
[3] Baeg, K. J., Caironi, M., & Noh, Y. Y. (2013). *Adv. Mater.*, *25*, 4210.
[4] Hauser, J. R. (1993). *IEEE Trans. Educ.*, *36*, 363.
[5] Risteska, A., Chan, K. Y., Anthopoulos, T. D., Gordijn, A., Stiebig, H., Nakamura, M., & Knipp, D. (2012). *Org. Elec.*, *13*, 2816.
[6] Burns, S. E., Cain, P., Mills, J., Wang, J. Z., & Sirringhaus, H. (2003). *MRS Bull*, *28*, 829.
[7] Javey, A., Wang, Q., Ural, A., Li, Y. M., & Dai, H. J. (2002). *Nano lett.*, *2*, 929.
[8] Loo, Y. L., Someya, T., Baldwin, K. W., Bao, Z., Ho, P., Dodabalapur, A., Katz, H. E., & Rogers, J. A. (2002). *Proc. Natl. Acad. Sci. USA*, *99*, 10252.
[9] Baeg, K. J., Khim, D., Kim, D. Y., Jung, S. W., Koo, J. B., You, I. K., Yan, H., Facchetti, A., & Noh, Y. Y. (2011). *J. Polym. Sci. B Polym. Phys.*, *49*, 62.
[10] Khim, D., Han, H., Baeg, K. J., Kim, J., Kwak, S. W., Kim, D. Y., & Noh, Y. Y. (2013). *Adv. Mater.*, *25*, 4302.
[11] Bijleveld, J. C., Zoombelt, A. P., Mathijssen, S. G. J., Wienk, M. M., Turbiez, M., de Leeuw, D. M., & Janssen, R. A. J. (2009). *J. Am. Chem. Soc.*, *131*, 16616.
[12] Hong, W., Sun, B., Aziz, H., Park, W. T., Noh, Y. Y.,& Li, Y. (2012). *Chem. Commun.*, *48*, 8413.
[13] Chen, Z., Zheng, Y., Yan, H., & Facchetti, A. (2009). *J. Am. Chem. Soc.*, *131*, 8.
[14] Baeg, K. J., Kim, J., Khim, D., Caironi, M., Kim, D. Y., You, I. K., Quinn, J. R., Facchetti, A., & Noh, Y. Y. (2011). *ACS Appl. Mater. Interfaces*, *3*, 3205.